Kβ-Detected XANES of Framework-Substituted FeZSM-5 Zeolites

Willem M. Heijboer,[†] Pieter Glatzel,[†] Kaveri R. Sawant,[‡] Raul F. Lobo,[‡] Uwe Bergmann,[§] Raul A. Barrea,[#] Diek C. Koningsberger,[†] Bert M. Weckhuysen,[†] and Frank M. F. de Groot*[,†]

Department of Inorganic Chemistry and Catalysis, Debye Institute, Utrecht University, Sorbonnelaan 16, 3584 CA Utrecht, The Netherlands, Department of Chemical Engineering, Center for Catalytic Science & Technology, University of Delaware, Newark, Delaware 19716, Stanford Synchrotron Radiation Laboratory, 2575 Sand Hill Road, Menlo Park, California 94025, and Argonne National Laboratory, Advanced Photon Source, BioCAT, Argonne, Illinois 60439

Received: April 14, 2004; In Final Form: April 28, 2004

The valence and local symmetry of iron in framework-substituted FeZSM-5 with a high Fe dilution (Si/Fe = 360) was studied by means of Kβ-detected X-ray absorption spectroscopy. This technique combines high-resolution ($\Delta E \sim 1$ eV) fluorescence detection of the 3p to 1s (Kβ) transition with the X-ray absorption near-edge structure (XANES) at the Fe K-edge. An absorption-like spectrum is recorded by detecting the Kβ fluorescence intensity as a function of the incident energy that is scanned through the K absorption edge. Kβ-detected XANES spectra allow for a more precise separation of the weak K pre-edge structure from the main edge as compared to conventional absorption spectroscopy. Subsequent analysis and interpretation of the pre-edge spectral features therefore is more accurate. The pre-edge is sensitive to changes in the local coordination and oxidation state of Fe. Using this technique we were able to quantitatively determine the degree of iron extraction out of a zeolite framework upon steaming. With the use of appropriate reference compounds, the pre-edge analysis was used to monitor the activation of low-loaded, framework-substituted FeZSM-5 (0.3 wt % Fe). Template removal and calcination distort the zeolite framework and induce a deviation from T_d symmetry for incorporated iron. The (deliberate) presence of water at high temperature ($T > 500$ °C) facilitates the hydrolysis of the Si−O−Fe bonds and increases the formation of extraframework iron species. The amount of Fe^{III} occupying tetrahedral sites in the MFI-type zeolite decreases to 32% and 19%, respectively, for mild- and hard-steamed samples.

1. Introduction

Oxygen transfer reactions are very important in catalysis, as they are in nature. A wide range of transition metals are able to catalyze such reactions. The activity, selectivity, and stability of the catalytically active species strongly depend on their structure and local environment. Zeolites have proven to be good hosts for active species of transition metals. The metal elements can either be introduced during the zeolite synthesis or through postsynthesis treatments. In recent years, FeZSM-5 has attracted much attention because of its ability for selective oxidation of hydrocarbons and its ability for the catalytic conversion of nitrogen oxides.[1] The specific activity for a certain reaction is largely determined by the way in which the FeZSM-5 catalyst is prepared. For example, the activity of framework-substituted FeZSM-5, with an Fe content below 1 wt %, for the catalytic decomposition of nitrous oxide and its use as an oxidant for the one step selective oxidation of benzene to phenol has been shown by Panov and co-workers[2] and by others.[3,4] Conversely, over-exchanged Fe/ZSM-5 with a much higher concentration of iron, introduced via postsynthesis methods, is an effective catalyst for the reduction of nitrogen oxides by hydrocarbons[5,6] or ammonia.[7] To distinguish the postsynthesis introduction of iron in ZSM-5, we use Fe/ZSM-5 instead of FeZSM-5.

For both types of FeZSM-5 catalysts the specific catalytic activity is well established, but the nature of the active sites involved is still under debate. The exclusive preparation of the active phase on a catalyst is often infeasible, as is the case for FeZSM-5. Unraveling the structure of the active species becomes therefore a complicated task. With the use of extended X-ray absorption fine structure (EXAFS) studies it was possible to reveal that in over-exchanged Fe/ZSM-5, prepared by chemical vapor deposition of $FeCl_3$, the majority (ca. 70%) of the iron is present in active binuclear iron clusters.[8,9] These Fe_2O_2 diamond core structures bear a close resemblance to the active site of enzymes such as methane monooxygenase (MMO). Also for CuZSM-5 the existence of such an M_2O_2 diamond core site has been reported.[10]

The activation of low-loaded framework-substituted FeZSM-5 mostly yields a very heterogeneous system. Heating in a flow of air or oxygen (calcination) especially in the presence of water vapor (steaming) extracts the iron, originally in the tetrahedral sites of the zeolite structure (MFI-type), into extraframework positions. Usually a variety of species is formed: isolated extraframework Fe oxo-ions (Fe_1), binuclear oxo-iron complexes (Fe_2), and oligonuclear oxo-iron complexes (Fe_N) located in the zeolite channels in addition to—catalytically inactive—larger iron oxide nanoparticles on the external surface of the zeolite (FeO_x).[3] Moreover, part of the iron stays in the framework in inverse relation to the severity of the activation treatment.

However, the current techniques employed for the characterization of FeZSM-5 are not well suited to determine the ratio

* Corresponding author. E-mail: F.M.F.deGroot@chem.uu.nl.
[†] Utrecht University.
[‡] University of Delaware.
[§] Stanford Synchrotron Radiation Laboratory.
[#] Advanced Photon Source.

10.1021/jp048368w CCC: $27.50
Published on Web 00/00/0000 PAGE EST: 9.4

between iron in tetrahedral (framework) and octahedral (extra-framework) coordination sites. For instance, Mössbauer and EXAFS spectroscopy can prove qualitatively the presence of iron in a specific coordination but are in general not able to provide a quantitative analysis for mixtures. An exception is a detailed EXAFS study concerning the well-defined case of $CuCl_2/Al_2O_3$ catalysts that contain mixtures of different phases with known geometry but with varying mutual ratios depending on the Cu loading.[11] However, in the present study on Fe-containing zeolites not only the large heterogeneity of the species formed but, moreover, the very low concentration of Fe in framework-substituted Fe/ZSM-5 complicates the use of the above-mentioned techniques.

We use Kβ-detected XANES (X-ray absorption near-edge structure) to probe quantitatively the local symmetry of Fe. The pre-edge feature of the Fe K-edge X-ray absorption spectrum is sensitive to the electronic structure of the iron site. The pre-edge arises from transitions of an Fe 1s electron into the lowest unoccupied electronic states that mainly have Fe 3d character. In a centrosymmetric system those transitions are dipole forbidden and therefore have in general very low intensity. However, a deviation from a centrosymmetric environment enables the mixing of 3d with 4p orbitals. Due to this hybridization some electric dipole allowed 1s $\rightarrow$ 4p character is added to the 3d-band transitions, resulting in an enhanced intensity of the pre-edge structure. Thus, iron in a noncentrosymmetric tetrahedral symmetry gives rise to a much more intense Fe K-edge pre-edge than in a centrosymmetric octahedral symmetry. Therefore, changes in the pre-edge intensity reflect the changes in the local coordination sphere (geometry) of Fe. In addition, the energy position of the pre-edge is related to the oxidation state of Fe, in other words, the occupation of the 3d band.[12]

The main requirements for a quantitative determination of changes in the coordination of iron based on variations of the pre-edge features are (1) a high resolution of the spectra so that characteristic features in the pre-edge are well resolved, (2) a precise isolation of the pre-edge structure from the main edge, which requires a proper background subtraction, and (3) the choice of relevant parameters to describe the pre-edge characteristics. Lately, several groups have used XANES to study the local coordination of iron in over-exchanged Fe/ZSM-5.[9,13−16] Lamberti and co-workers reported on the characterization of aluminum-free Fe-silicalite, which has a similar MFI zeolite structure as ZSM-5.[17−21] Using Fe K-edge XANES they investigated the influence of template removal and calcination on the coordination and oxidation state of iron initially incorporated in Fe-silicalite. The authors described the characteristics of the pre-edge feature by means of peak position and intensity but did not separate the contribution from the main absorption edge to the pre-edge feature.

In a detailed and extensive XANES study on Fe-bearing minerals Wilke and co-workers[22] presented a correlation of the changes of the Fe K pre-edge with the oxidation state and local symmetry. The pre-edge features of Fe in more than 30 minerals and synthetic compounds were systematically studied. The most useful characteristics of the pre-edge feature were the energy position of the centroid and its integrated intensity. Also Westre and co-workers[12] have proven for ferrous and ferric model compounds that these are the appropriate parameters to unambiguously characterize the pre-edge feature. In previous *in situ* Kβ-detected high-resolution XANES studies, Battiston et al.[8,23,24] used the findings of Wilke et al. obtained for binary mixtures of $^{[6]}Fe^{III}/^{[4]}Fe^{II}$ to understand the evolution and reactivity of binuclear Fe complexes in over-exchanged Fe/ZSM-5 upon heating in He and in O_2.

However, the spectra in the study by Battiston et al. show a lower energy resolution that is essentially the same as for conventional XANES measurements. In addition, they show rather poor signal-to-noise ratios at Fe loadings that are higher by a factor of 15 than those in the present study. Because of the poor energy resolution, the pre-edge analysis utilizes a cubic spline function because of the background, that is, a tailing contribution of main edge to pre-edge, because the pre-edge is still not well separated from the main edge. The use of a cubic spline function introduces a significant error as we will show below. Due to these experimental limitations the study by Battiston et al. did not allow for a detailed quantitative analysis.

In this work, we present a study of the Fe K pre-edge region in low-loaded, framework-substituted FeZSM-5 by means of Kβ-detected XANES spectroscopy. The pre-edge spectral features represent excited electronic states of the Fe ion where a 1s electron has been elevated to a low-lying unoccupied state by an incoming X-ray photon. The Kβ fluorescence is emitted when the hole in the 1s shell is subsequently filled by a 3p electron. A high-resolution Kβ spectrum can be measured using a crystal spectrometer with an energy bandwidth of about 1 eV. The Kβ fluorescence intensity depends on the probability of exciting a 1s electron, that is, it depends on the absorption cross section at the K-edge. By detecting the Kβ intensity as a function of the incident energy it is thus possible to record absorption-like spectra.[25−27]

The advantage of high-resolution Kβ-detected XANES spectroscopy is that it shows spectral features that are sharper than in conventional absorption spectroscopy recorded in transmission mode or by fluorescence detection using a solid-state detector with medium energy resolution (e.g., Ge: $\Delta E \sim$ 200 eV). We show that high-resolution Kβ-detected XANES spectra allow for a more precise background subtraction and consequently a higher accuracy in determining the local geometry and oxidation state of Fe in ZSM-5. The application of this technique enables a quantitative determination of the degree of iron extraction out of the zeolite matrix which is not possible using other techniques. We point out that in this study X-ray absorption data are presented for the first time on an FeZSM-5 catalyst with an Fe loading fairly well below 1 wt %, which was the limit so far, even for a qualitative analysis.[20]

2. Experimental Section

2.1. Catalyst Preparation and Characterization. *2.1.1. Framework-Substituted FeZSM-5.* This material was prepared via the hydrothermal synthesis method.[4] FeZSM-5, with Si/Al = 36 and Si/Fe = 175 ratios in the starting synthesis mixture, was prepared according to the procedure described below. The synthesis mixture contained tetraethylorthosilicate (TEOS, Aldrich, 99+%, tetrapropylammonium hydroxide (TPAOH, Alfa Aaeser, 40%w/w in water), iron (III) sulfate (VWR), aluminum nitrate nonahydrated (Aldrich, 99.99%), and sodium hydroxide (VWR) in the following nominal molar ratios: H_2O/Si = 45, TPAOH/Si = 0.1, NaOH/Si = 0.2, Si/Al = 36, and Si/Fe = 175.

In a typical synthesis, the silica source (TEOS) was added to the organic template (TPAOH) and sodium hydroxide while being vigorously stirred. Drops of this solution were added to a mixture of iron sulfate and aluminum nitrate dissolved in water. The final solution was transferred to a stainless steel autoclave and kept in a static air oven at 190 °C for 5 days. The crystalline material was separated by filtration, washed with

approximately 2 L of DI water or until the product was color-free, and dried at room temperature overnight (denoted as catalyst *am*-FeZSM-5). The samples were characterized with powder X-ray diffraction to confirm the structure and purity of the sample and elemental analysis by X-ray fluorescence (XRF) for relative ratios of Si, Al, and Fe (45.1, 1.17, 0.3 wt % respectively: Si/Fe ∼ 360 and Si/Al ∼ 37).

The template was removed carefully from the as-synthesized sample (*am*) by pyrolysis in a dried nitrogen flow of 50 mL/min at 520 °C (heating rate 1 °C/min) for 2 h and consecutive calcination in a dry airflow of 100 mL/min at 520 °C (2 °C/min) for 2.5 h *(tf*-FeZSM-5). The samples were converted into the NH_4 form by exchange with an ammonium nitrate solution (0.1 M) overnight at 70 °C. The sample was filtered and dried for 2 h at 60 °C (*NH_4*-FeZSM-5). The H form was obtained by calcination in a dry airflow of 100 mL/min at 520 °C (2 °C/min) for 1 h (*H*-FeZSM-5). In the last step, the catalysts were steamed, in two different ways. First a hard-steaming procedure was carried out, according to literature,[4] with a water partial pressure of 300 mbar in a total flow of 30 mL/min of nitrogen at a high temperature of 600 °C for 5 h (*hs*-FeZSM-5). In addition, we performed a mild-steaming procedure with a water partial pressure of 200 mbar in a total flow of 200 mL/min of nitrogen at a high temperature of 550 °C for 4 h (*ms*-FeZSM-5). The samples were stored at room temperature in dry air.

2.1.2. Over-Exchanged Fe/ZSM-5. This material was prepared following the $FeCl_3$ sublimation technique (also called chemical vapor deposition (CVD)), proposed by Chen and Sachtler[5] and described in more detail by Battiston and co-workers.[8] The H^+ removal efficiency (98%), determined by HCl titration, indicated that during the Fe-exchange procedure nearly all the Brönsted acid sites were removed from the H/ZSM-5.

Fe/ZSM-5 was calcined by heating to 200 °C in a PFR reactor under a specific He flow of 800 mL/min·g and with a moderate temperature ramp (0.5 °C/min). At this temperature, 200 mL/min·g of O_2 was added to the He flow while, under the same temperature ramp, heating was continued to 550 °C. After 3 h at 550 °C, the temperature was decreased to 30 °C. The crystalline fingerprint of the zeolitic support was monitored after each synthesis step by XRD. On the basis of these measurements lattice damage or formation of large iron oxides phases could be excluded, even upon calcination. Elemental analysis by inductively coupled plasma (ICP) was carried out to determine the silicon/aluminum ratio (Si/Al = 17.0) and the iron loading (Fe/Al = 0.97, 4.4 wt % Fe) of the obtained Fe/ZSM-5.

2.2. Kβ-Detected XANES. *2.2.1. Experimental Setup.* The Kβ-detected XANES spectra were measured at beamline 18-ID (BioCAT) at the Advanced Photon Source of the Argonne National Laboratories (Chicago). The energy of the incoming synchrotron beam was selected by means of a Si(111) double-crystal monochromator. The incident beam was guarded by a 0.5 mm vertical by 1 mm horizontal slit in front of the sample. The energy bandwidth of the incident X-ray beam was approximately 1.2 eV at 7100 eV and the (maximum) incident flux was 10^{13} photons/s, as monitored by a helium-filled ionization chamber downstream of the guarding slit. The incident energy was calibrated using tabulated values for the K-edge features of an Fe foil standard. By repeatedly measuring the standard we determined a relative error of 0.1 eV for the incident energy. A focusing mirror rejected higher harmonics.

The fluorescence emission from the sample was collected by a crystal array spectrometer,[28] using six spherically bent Ge(620) crystals with a bending radius of 860 mm. The six analyzer crystals have a diameter of 44 mm, yielding a solid angle of approximately 0.013 sr. A Ge solid-state detector was placed at the common focus of the six crystals. To avoid unwanted X-ray photons, the energy window of the Ge detector was set to ∼600 eV and an additional slit was positioned just in front of the detector. The analyzer energy resolution is approximately 1.0 eV at the iron Kβ emission. The relative energy calibration of the emission spectrometer is sensitive to vertical movements of the synchrotron beam. The energy calibration was repeatedly checked with the Kβ emission of an Fe_2O_3 sample and was found to be constant within 0.1 eV (relative emission energy error). We give an absolute error for the emission energy scale of 1 eV.

High-resolution Kβ-detected XANES spectra were recorded by tuning the emission analyzer energy to the maximum intensity of the Fe Kβ lines of Fe_2O_3 and by scanning the incident energy through the XANES region. This procedure is referred to as a constant emission energy (CEE) scan. In Figure 1 we give a schematic representation of the detection setup as well as an Fe Kβ emission spectrum in which the spectral area is indicated that is selected out of the fluorescence by using the high-resolution detector. The maximum of the Kβ emission for Fe^{III} (Fe_2O_3) was calibrated at 7059.3 eV, and a relative shift of 0.3 eV to lower emission energy was observed for Fe^{II} (Fe_2SiO_4). The same emission energy was used for all FeZSM-5 measurements, and the CEE scans were therefore not necessarily taken in the maximum of the Kβ main peak. The Kβ intensity changes by approximately 5% within 0.3 eV. However, the pre-edge intensity normalized to the main edge will hardly change because the Kβ peak shift affects the pre-edge and the main edge. The small error introduced by different Kβ peak shifts between pre-edge and main edge is estimated to be less than 2%. Conventional absorption spectra were obtained by integrating the Kβ fluorescence over 25 eV. This corresponds to recording the total 3p to 1s fluorescence yield, which gives a good approximation to a conventional absorption spectrum.

2.2.2. Data Acquisition. The Fe/ZSM-5 samples were pressed into self-supporting wafers and placed in an *in situ* fluorescence cell at a 45° scattering angle with respect to the incoming beam.[29] Spectra were recorded at 1 bar during heating treatments from 25 to 350 °C (heating ramp of 5 °C/min). The heating treatments were performed in moderate oxygen atmospheres, that is, a flowing mixture of 7.7% O_2 in He (total flow 100 mL/min). After stabilization at 350 °C XANES spectra were taken. After switching to helium atmosphere this sequence was repeated as was done for some samples in oxygen at room temperature after cooling. Hematite, fayalite and iron(III) phosphate were measured under air at 25 °C as references.

2.2.3. Data Processing. The Kβ-detected Fe XANES spectra were normalized by the average absorption intensity, as determined at around 7200 eV. The complete spectrum was modeled by using the software PeakFit4 (AISN Software, 1995). A typical spectrum could be simulated by a Gauss cumulative ascending function for the main edge combined with a pseudo-Voigt peak. Voigt profiles combine Lorentzian and Gaussian functions and hence account for, respectively, lifetime and experimental broadening. The pre-edge spectral shape has been fitted with a good R-squared value ($R^2 > 0.999$) using as few components as possible.

The conventional XANES spectra were also normalized by the average absorption intensity as determined at around 7200 eV. After normalization, the pre-edge feature was isolated by subtraction of the main Fe K absorption edge contribution. The contribution of the main edge was calculated for the whole energy range using a cubic spline function, while the data several

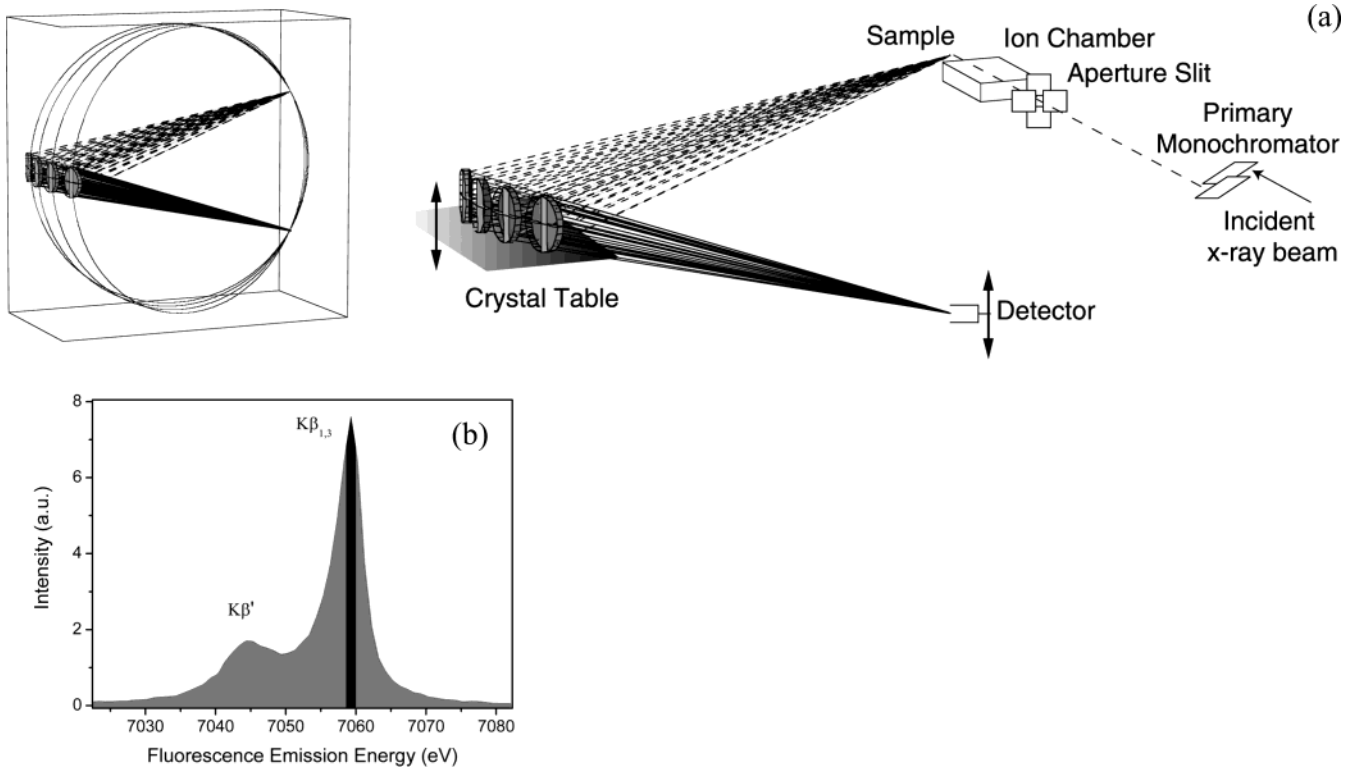

Figure 1. (a) Diagram of the high-resolution fluorescence crystal array spectrometer, using six spherically bent Ge(620) crystals to collect the Fe Kβ region with ~1.0 eV resolution. The inset (left) shows the orientation of the Rowland circles for each analyzer crystal. (b) The integrated intensity given by the black energy window of ~1.0 eV is selected out of the Fe 3p to 1s X-ray fluorescence emission (gray), which is emitted upon core hole relaxation after 1s electron excitation.

eV before and after the energy position of the pre-edge were used to interpolate the main edge at the pre-edge energy position.[22]

The characteristics of the isolated pre-edges, centroid energy position and integrated intensity, were calculated using the peak-fitting results of the pre-edge feature. The energy position of the centroid is defined as the center of gravity of the (pseudo-Voigt) components. The contribution from components centered above 7115.0 eV was ignored.[22,23] The obtained centroid positions have been calibrated to the reported values of Wilke and co-workers, which results in a shift to lower energy of 0.77 eV.

3. Results

3.1. Fe Kβ-Detected XANES versus Normal XANES. *3.1.1. Pre-edge Isolation.* Figure 2 shows the pre-edge region of the Fe K-edge X-ray absorption spectrum of Fe_2SiO_4 (fayalite) measured in two different ways. The bottom portion of Figure 2 shows the Fe K pre-edge structure in a conventional absorption spectrum. The contribution of the main Fe K-edge in the pre-edge region was determined by using a cubic spline function, obtained by interpolating the data several electronvolts before and after the pre-edge (dashed line). The subtraction of the modeled main edge contribution from the XANES spectrum—over the full energy range—yields the isolated pre-edge feature. The pre-edge intensity for the spectra measured by normal XANES strongly depends on the subtracted cubic spline function. We estimated the error of this procedure by performing several cubic spline fits using various energy ranges around the pre-edge energy position. We experienced with a series of cubic spline functions, which in principle were all appropriate to model the background, that the variation in the resulting integrated pre-edge intensity amounts to 20% for compounds with a weak

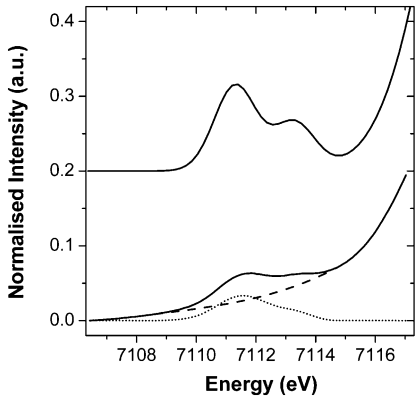

Figure 2. Fe K pre-edge feature of Fe_2SiO_4 (fayalite: Fe^{II}, O_h). Below: conventional fluorescence XANES spectrum (solid), cubic spline function used to model the background (dash), and the isolated pre-edge (dot), analysis according Wilke et al.[22] Top: Kβ-detected XANES spectrum, no background subtracted. In both spectra the pre-edge is normalized to the average absorption intensity calculated around 7200 eV.

pre-edge (i.e., with an octahedral oxygen coordination). Reference spectra, which are analyzed in exactly the way, provide a framework for the determination of the variance introduced by the analysis method. However, despite this improvement, we expect this procedure to be still susceptible to a certain lack of reproducibility. To overcome this disadvantage of normal XANES we measured the spectra by means of Kβ-detected XANES.

The top portion of Figure 2 shows the Fe_2SiO_4 spectrum measured by Kβ-detected constant emission energy (CEE) scans, denoted as Kβ-detected XANES. The small fluorescence energy window selected by the high-resolution detector used in this experiment suppresses the background contribution due to

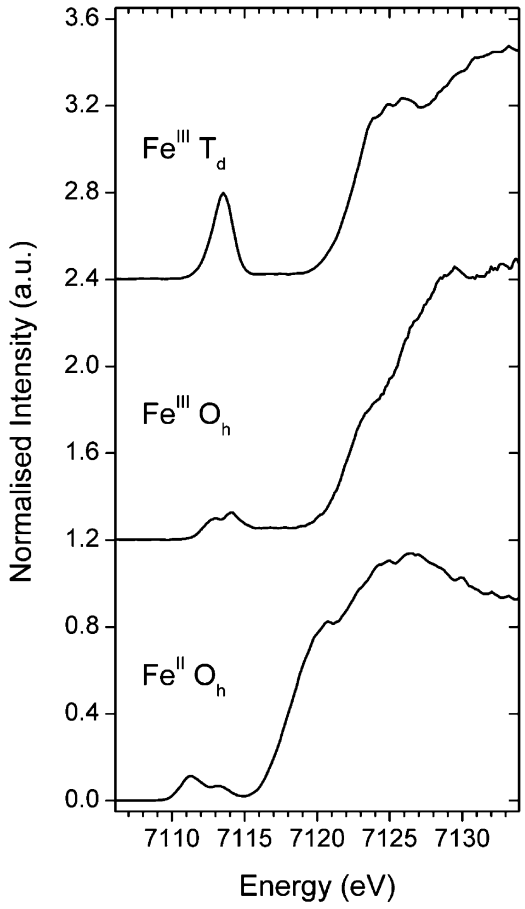

Figure 3. Kβ-detected XANES of selected iron oxide model compounds, from top to bottom: $FePO_4$, iron phosphate (Fe^{III} in tetrahedral oxygen coordination), α-Fe_2O_3, hematite (Fe^{III} in octahedral oxygen coordination), and Fe_2SiO_4, fayalite (Fe^{II} in octahedral oxygen coordination).

lifetime broadening of the main edge. This results in an almost flat signal before the pre-edge. Therefore, no background is subtracted from the Kβ-detected XANES. Figure 2 shows that the peaks in the pre-edge feature measured by Kβ-detected XANES are much better separated from the main edge. Furthermore, we find that the Kβ-detected pre-edge structures show a significantly higher integrated intensity relative to the normalized main edge.

3.1.2. Fe Oxide Model Compounds. Figure 3 shows the Kβ-detected XANES spectra of Fe_2SiO_4 (fayalite: Fe^{II} in O_h), α-Fe_2O_3 (hematite: Fe^{III} in O_h), and $FePO_4$ (iron phosphate: Fe^{III} in T_d). $FePO_4$ exhibits a sharp and strong pre-edge peak—as an almost perfect model for Fe in a tetrahedral coordination of oxygen. The much weaker prepeaks of α-Fe_2O_3—Fe in nonperfect octahedral oxygen coordination—are also clearly visible. The low spectral intensity between the pre-edge and the main edge in α-Fe_2O_3 has been attributed to Fe−Fe contributions.[22] Fe_2SiO_4—as an Fe^{II} model compound with octahedral oxygen coordination—exhibits a different spectral shape of the pre-edge, which is also shifted to lower energy by ∼1.5 eV relative to the energy position of α-Fe_2O_3. The position of the main edge shifts by ∼4 eV relative to the energy position of the Fe^{3+} oxide compounds. This difference in the relative energy shifts is in line with the general observations that pre-edges shift less than edges.[12]

Table 1 lists the characteristics of the pre-edge spectral features, that is, the energy positions of the fitted peaks, the centroid of the pre-edge structure, and the integrated intensities.

TABLE 1: Pre-Edge Characteristics for Reference Compounds, Fe_2SiO_4 (Fe^{II}, O_h), Fe_2O_3 (Fe^{III}, O_h), and $FePO_4$ (Fe^{III}, T_d)

sample − detection[a]	component position (eV)	area	centroid (eV)	total area
Fe_2SiO_4 − Kβ[b]	7111.31	0.2020	7112.02	0.3161
	7113.28	0.1141		
Fe_2SiO_4 − proc Wilke[c]	7110.83	0.0197	7111.85	0.0851
	7111.70	0.0440		
	7113.10	0.0214		
Fe_2SiO_4 − ref Wilke[d]	7111.22	0.0385	7112.04	0.1025
	7111.81	0.0313		
	7113.24	0.0327		
Fe_2O_3 − Kβ	7112.74	0.1239	7113.59	0.2886
	7114.22	0.1647		
	7116.01[e]	0.0581[e]		
	7117.60[e]	0.0418[e]		
Fe_2O_3 − proc Wilke	7112.65	0.0355	7113.50	0.0926
	7114.02	0.0571		
	7115.50[e]	0.0274[e]		
	7116.87[e]	0.0181[e]		
Fe_2O_3 − ref Wilke	7112.68	0.0489	7113.47	0.1236
	7113.98	0.0747		
	7115.22[e]	0.0468[e]		
	7116.68[e]	0.0332[e]		
	7117.83[e]	0.0109[e]		
$FePO_4$ − Kβ	7112.73	0.1561	7113.45	0.8039
	7113.62	0.6478		
$FePO_4$ − proc Wilke	7113.52	0.2500	7113.52	0.2500
$FePO_4$ − ref Wilke	7113.55	0.3423	7113.55	0.3423

[a] Samples measured at 25 °C in air. [b] Spectra measured by Kβ-detected XANES. [c] Spectra measured by conventional fluorescence yield XANES, analysis according to Wilke et al.[22] [d] Literature data from Wilke et al.[22] [e] Contribution above 7115 eV not included in centroid.

The latter two numbers do not include peaks above 7115 eV, because these peaks are supposedly due to Fe−Fe interactions. For each compound, we show the values as obtained from the Kβ-detected and conventional XANES as well as the numbers reported by Wilke et al.[22] There is good agreement for the numbers obtained from conventional XANES between our data and these results. On the other hand, in the Kβ-detected XANES spectra the intensity (total area) of the pre-edge is approximately 3 times higher than in the conventional XANES spectra. The systematic increase of the pre-edge intensity with respect to the edge jump is related to the fact that the fluorescence energy selected by the detector is set at the maximum intensity of the Kβ emission on the pre-edge (using Fe_2O_3). The determination of this setting during resonant excitation at the pre-edge causes an enhanced pre-edge intensity relative to the main edge jump. This accounts for the systematically higher pre-edge to main edge intensity ratio for Kβ-detected XANES compared to conventional XANES.

While the amount and energy position of the different peaks that contribute to the pre-edge feature deviate between the two detection modes, we obtain the same centroid positions. Figure 4 is a graphical summary of the data in Table 1. The dotted vertical lines indicate the average energy position of the centroids representing Fe^{II} and Fe^{III} compounds at 7112.0 and 7113.5 eV, respectively.

3.2. Activation of Framework-Substituted FeZSM-5. The influence of the activation treatments on the oxidation state and local geometry of iron in framework-substituted FeZSM-5 is probed by Kβ-detected XANES. In Figure 5 the spectra in the energy region of 7105−7135 eV are shown for FeZSM-5 samples after template decomposition (*tf*-FeZSM-5), calcination, ion exchange, and again calcination (*H*) and steaming (*ms*/*hs*).

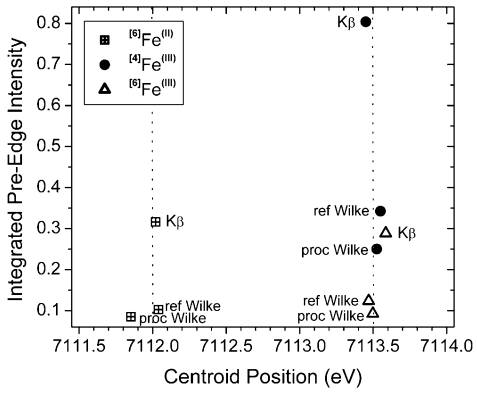

Figure 4. Integrated pre-edge intensity vs centroid position for Fe in selected model compounds, characteristics denoted by $^{[\text{O-coordination}]}\text{Fe}^{(\text{formal valence})}$: $FePO_4 = {}^{[4]}Fe^{(III)}$, $\alpha\text{-}Fe_2O_3 = {}^{[6]}Fe^{(III)}$, and $Fe_2SiO_4 = {}^{[6]}Fe^{(II)}$. Dotted vertical lines at 7112.0 and 7113.5 eV indicate the average energy position of the centroid for Fe^{II} and Fe^{III} compounds, respectively. The different methods are (Kβ) Kβ-detected XANES, (proc Wilke) total fluorescence XANES using the edge subtraction procedure outlined by Wilke and co-workers, and (ref Wilke) data as reported by Wilke et al.[22]

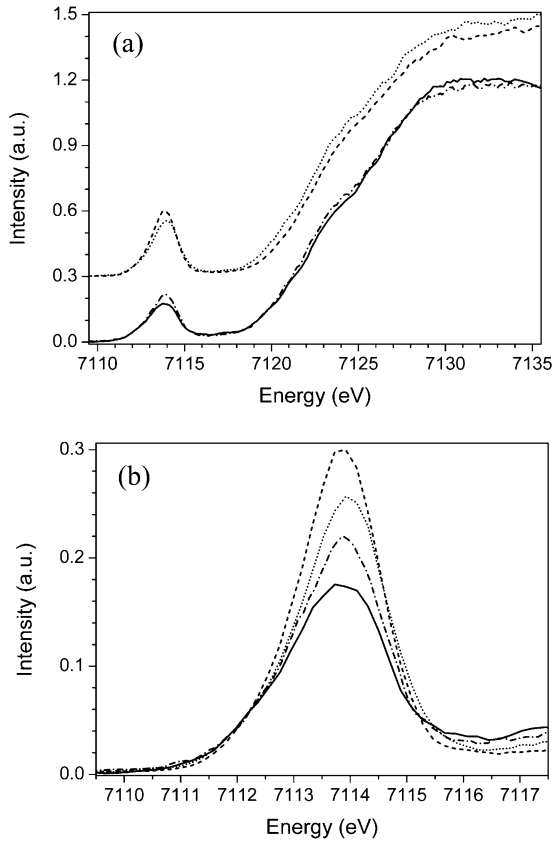

Figure 5. (a) Kβ-detected XANES of framework-substituted FeZSM-5 samples: *tf*-FeZSM-5, after template removal (dashed line); *H*-FeZSM-5, proton form after calcination of ammonium-exchanged sample (dotted line); *ms*-FeZSM-5, mild-steamed sample (dash-dot line); and *hs*-FeZSM-5, hard-steamed sample (solid line). The spectra were measured in a flow of oxygen (7.7 vol % in He) at 350 °C. (b) Zoom of the pre-edge region.

The pre-edge region is enlarged to facilitate the comparison of the intensities of the different spectra. The samples were all measured at 350 °C in moderate oxygen atmosphere, that is, 7.7% O_2 in He. No spectra were recorded for as-made (*am*) and ammonium-form (NH_4) FeZSM-5 samples. The energy position of the pre-edge does not change. The intensity of the pre-edge peak, however, is clearly influenced by each activation step. We note that after the removal of the template by pyrolysis in dry nitrogen at 520 °C, the sample was calcined in dry air, then ammonium exchanged, and finally a second calcination in dry air was conducted to obtain the proton form (*H*). This treatment results in a decrease of the pre-edge intensity, from 0.64 to 0.55 (see Table 2). A further decline of the pre-edge intensity is observed upon steam treatment. The total area amounts to 0.46 and 0.39, respectively, for mild-steamed (*ms*) and hard-steamed samples (*hs*).

TABLE 2: Pre-Edge Characteristics for FeZSM-5 Samples (Kβ-Detected XANES)[a]

sample[b]	treatment	component position (eV)	area	centroid (eV)	total area
am-FeZSM-5	as synthesized				
tf-FeZSM-5	template free	7112.85	0.1038	7113.74	0.6402
		7113.92	0.5364		
NH_4-FeZSM-5	ammonium exchanged				
H-FeZSM-5	calcined	7112.73	0.0917	7113.78	0.5459
		7114.00	0.4543		
H-FeZSM-5[c]	calcined	7111.89	0.0285	7113.74	0.3383
		7113.91	0.3099		
ms-FeZSM-5	mild steamed	7112.76	0.0935	7113.71	0.4550
		7113.95	0.3615		
hs-FeZSM-5	hard steamed	7112.78	0.0906	7113.68	0.3887
		7113.95	0.2981		
cvd-Fe/ZSM-5	calcined	7112.59	0.0360	7113.58	0.4456
		7113.67	0.4096		
		7116.35[d]	0.0666[d]		
cvd-Fe/ZSM-5[c]	calcined	7112.94	0.0476	7113.64	0.3227
		7113.77	0.2751		
		7116.68[d]	0.0359[d]		

[a] *am*-FeZSM-5 and NH_4-FeZSM-5 are not measured. [b] Measured at 350 °C in O_2 (7.7% in He) unless stated otherwise. [c] Measured at 25 °C after measurements at 350 °C and cooling. [d] Contribution above 7115 eV not included in centroid.

Because of the more uniform way of preparation of over-exchanged *cvd*-Fe/ZSM-5, its structure and reactivity is much better described in the literature. To obtain qualitative information on the behavior of activated framework FeZSM-5 we compare the proton form (*H*) with extraframework iron-containing over-exchanged *cvd*-Fe/ZSM-5. Kβ-detected XANES spectra were subsequently taken under oxygen (7.7% in He) at 25 °C and at 350 °C. In Figure 6 the spectra in the energy region of 7105−7135 eV are shown for *H*-FeZSM-5 and *cvd*-Fe/ZSM-5 (high-loaded sample, extraframework iron introduced via the chemical vapor deposition method). Spectra were furthermore taken under pure He at 350 °C (not shown). The pre-edge peak intensity at 350 °C is higher for framework-substituted *H*-FeZSM-5 indicating the presence of iron in tetrahedral positions, most probably of the zeolite lattice. Extraframework *cvd*-Fe/ZSM-5 does not have iron in the zeolite matrix (apart from small impurities), and the coordination of the iron atoms in the—predominantly present—binuclear clusters depends on the chemical environment. At 350 °C, under oxygen atmosphere, the coordination of oxygen around iron is most probably distorted from an octahedral arrangement, regarding the integrated pre-edge intensity, which is intermediate between the tetrahedral and octahedral reference iron oxide compounds[8] (see Figure 7). There is a small difference in the height of the pre-edge peak of *H*-FeZSM-5 measured under oxygen in helium and under pure helium. Upon cooling in the oxygen mixture both the low-loaded framework and the high-loaded extraframework sample display a lower pre-edge intensity. An additional spectral feature between the pre-edge and the main edge was

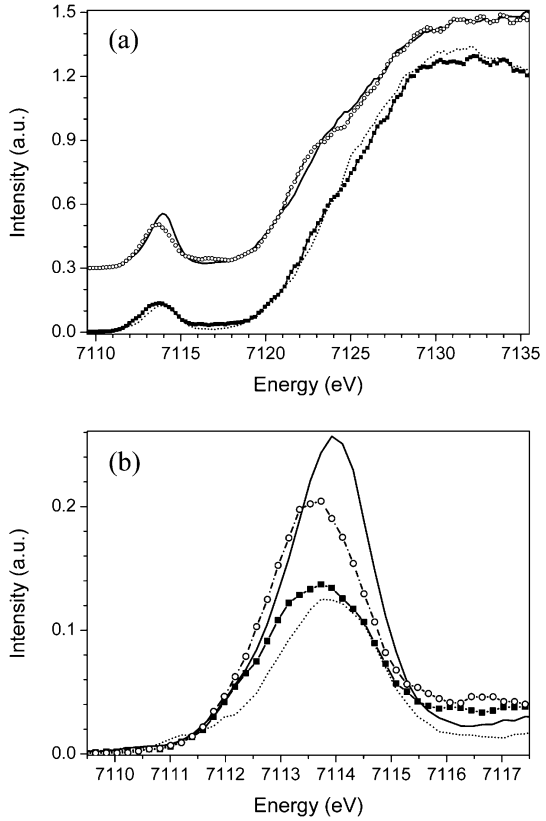

Figure 6. (a) Kβ-detected XANES of framework-substituted FeZSM-5 samples compared with extraframework Fe/ZSM-5 samples: *H*-FeZSM-5 in oxygen (7.7 vol % in He) at 25 °C (dotted line) and 350 °C (solid line); *cvd*-Fe/ZSM-5 in oxygen (7.7 vol % in He) at 25 °C (filled squares) and 350 °C (open circles). (b) Zoom of the pre-edge region.

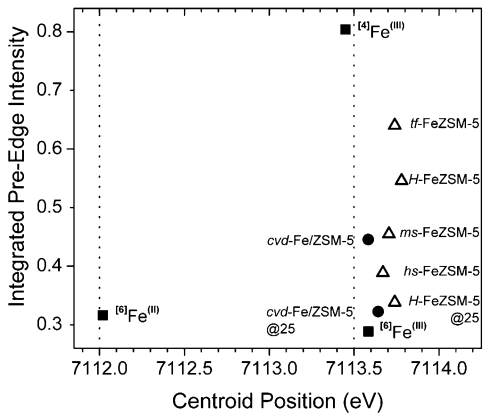

Figure 7. Integrated pre-edge intensity vs centroid position for iron in different FeZSM-5 samples. Framework-substituted FeZSM-5 samples are compared with extraframework *cvd*-Fe/ZSM-5 samples. All iron-containing ZSM-5 samples are measured in a flow of oxygen (7.7 vol % in He) at 350 °C unless indicated by @25, meaning 25 °C: *tf*-FeZSM-5, after template removal; *H*-FeZSM-5, proton form after calcination of ammonium-exchanged sample; *ms*-FeZSM-5, mild-steamed sample; and *hs*-FeZSM-5, hard-steamed sample. The pre-edge characteristics are also given for iron model compounds: $FePO_4$ = $^{[4]}Fe^{(III)}$, α-Fe_2O_3 = $^{[6]}Fe^{(III)}$, and Fe_2SiO_4 = $^{[6]}Fe^{(II)}$.

observed for extraframework *cvd*-Fe/ZSM-5. As noted before, this peak is believed to be due to Fe−Fe interactions.[22]

In Table 2 the pre-edge characteristics for the framework-substituted FeZSM-5 samples are listed. The pre-edge feature could be fitted best by two components. The first component at approximately 7112.8 eV has a smaller area, which remains constant during the treatments. Thus, the changes in the total area are related to the decrease in the integrated intensity of the second component around 7113.9 eV. A theoretical analysis and simulation study of Fe K-edge 1s → 3d pre-edge features of iron complexes reveals that for tetrahedral high-spin Fe^{III} compounds two components can be distinguished. The first one at lower energy is related to electric quadrupole transitions, and the second component originates from both quadrupole and dipole transitions.[12] As mentioned before, the enhanced pre-edge intensity for noncentrosymmetric systems is due to the dipole allowed 1s → 4p character added to the 3d band. The observed changes in the second component therefore clearly point to a change in symmetry. The valence of Fe is hardly affected regarding the unchanged intensities of the first component and rather similar energy positions of the whole centroid for the framework-substituted FeZSM-5 samples.

Figure 7 presents the changes in the centroid position and the integrated pre-edge intensity for framework-substituted (open triangles) and over-exchanged samples (filled circles). The characteristics of the reference iron oxide compounds with known valence and local coordination of iron are also plotted in the graph (filled squares). The energy position of the centroid does not differ much for the FeZSM-5 samples but deviates from the position of the Fe^{III} references by about 0.2 eV to higher energy.

4. Discussion

FeZSM-5 catalysts with a low loading of iron up to 1 wt % are most active and desirable for catalyzing the selective oxidation of benzene to phenol using N_2O as an oxidant.[1] A major reason for the use of framework-substituted iron-containing zeolites over the use of postsynthesis introduced ones is the lack of reproducibility of the latter type of low-loaded FeZSM-5. The type of iron species introduced by means of aqueous ion exchange, for instance, strongly depends on the pH of the solution and the nature of the counteranion. A pH close to 7 leads to the formation and precipitation of iron hydroxides and after calcination consequently to iron oxide clustering, most likely on the outer surface of the zeolite crystals. Ion exchange with some particular iron salts also tends to preferably cover the outer surface. Another issue is the stability of the iron anchored on the intrazeolitic cation-exchange positions.

To overcome these problems, it was suggested to introduce the active extraframework iron literally from the other side, that is, transform framework Fe into extraframework species. With the use of the hydrothermal synthesis method, Fe can be built in the silica matrix of MFI, yielding Fe-silicalite or, in the case of the presence of Al, FeZSM-5. Due to its larger dimensions the incorporation of an Fe atom most likely induces a local stress on the Si−O−Si bonds of the zeolite framework. The well-known hydrolysis of such bonds is probably enhanced for Fe−O−Si bonds. It is known that exposure to water indeed causes the extraction of Fe out of the tetrahedral framework positions. However, up to now, it has been impossible to quantify reliably the fraction of dislodged iron.

4.1. Quantitative Determination of Tetrahedral Fe. From the Kβ-detected XANES spectra the influence of activation treatments on the iron in framework-substituted FeZSM-5 is clearly visible. The maximum intensity of the pre-edge relative to the main edge is continuously decreasing upon progressive treatments from the as-made sample to the final steamed samples, while the peak shape remains rather similar. The integrated pre-edge intensity previously identified as a characteristic of the pre-edge shows the same downward trend. The

other defined pre-edge characteristic, the energy position of the centroid, hardly changes for the FeZSM-5 samples from the energy position for Fe^{III} compounds. To make a quantification of the amount of tetrahedral Fe, first the assumption is made that the symmetries of iron in $FePO_4$ and in Fe_2O_3 represent the extremes for the possible coordination of iron species in FeZSM-5, that is, isomorphous substitution for silicon in the T_d sites of the zeolite framework or fully extracted and hence 6-fold coordinated by oxygen. The integrated intensity of FeZSM-5 samples can now be considered as a linear combination of the two Fe^{III} references. We have chosen $FePO_4$ as a model for Fe^{III} in tetrahedral oxygen coordination and Fe_2O_3 as a model for Fe^{III} slightly distorted from octahedral oxygen coordination. Hereafter, the changes in the pre-edge will be discussed as modifications in the percentage of Fe^{III} occupying T_d sites, where $FePO_4$ is set to 100% and Fe_2O_3 to 0% Fe^{III} in T_d positions. This procedure is possible because the pre-edge integrated intensity is proportional to the probability of the 1s → 3d transitions, which in turn are related to the degree of distortion from the centrosymmetric coordination of the transition metal element, as is explained before. However, a small modification in the pre-edge intensity may arise from variations in the Fe−O bond distances. In a study on V K pre-edges of selected vanadium compounds Wong et al. found an "empirical relation" between the average bond distance and the product of the normalized peak height and width at half-height within each of the geometry types.[30]

4.2. Template Decomposition and Calcination. The use of the hydrothermal synthesis method aims at the incorporation of iron in the ZSM-5 framework structure. The spectrum for the as-synthesized sample at 350 °C was not measured in view of the presence of the carbonaceous template residue in the zeolite channels. We expect that the Fe coordination remains close to tetrahedral except for positions bound to the template. The next sample, template-free *tf*-FeZSM-5, was prepared by pyrolysis in dry nitrogen at 520 °C and a subsequent calcination in dry air at 520 °C. Together with the removal of the template out of the zeolite channels and cages, some iron might be extracted out of the framework as indicated by the decreased integrated pre-edge intensity for *tf*-FeZSM-5. If a low heating ramp (1 °C/min) and dried gases are used, the small extraction of iron should be induced by water produced during the template decomposition. Lamberti et al. reported previously[17−21] that for Fe-silicalite a "large fraction" of Fe migrates to extraframework positions upon template removal at 550 °C and calcination at 600 °C. In our case, most probably, the majority of the iron stays in a 4-fold oxygen coordination as derived from the integrated pre-edge intensity of 0.64 for *tf*-FeZSM-5.

The decrease in integrated intensity points to the distortion of the perfect tetrahedral geometry of the zeolite framework rather than to iron migration to extraframework positions. From the previously mentioned study of Wilke and co-workers[22] it is known that iron minerals in a 5-fold oxygen coordination display an integrated pre-edge intensity, which is between that of tetrahedral and octahedral coordination.[22] Distortion of the silicon−oxygen tetrahedrons upon template removal from the zeolite channels is promoted by the isomorphous substitution of silicon by the larger iron atoms. As long as the template is present the framework is stabilized, but for *tf*-FeZSM-5 the stress on the framework induced by the incorporated iron results in the apparent lowering of iron in "pure" T_d sites. An analogous relaxing influence of the synthesis template on the framework of molecular sieves was reported for cobalt atoms incorporated in $AlPO_4$-5.[31] Recently, Lamberti and co-workers presented a study on the template burning inside Fe-MFI using synchrotron-based X-ray powder diffraction.[32] Their experiment is somewhat different with respect to the sample (which is Al-free) and the more extreme conditions (the use of a pure oxygen flow and a relatively high heating rate of 7.2 °C/min from room temperature to 730 °C). Similar to our observations for *tf*-FeZSM-5 they noticed an increased disorder of the framework Si atoms upon template decomposition. This phenomenon is ascribed to rupture of Fe− or Si−O−Si bonds and partial Fe migration from the framework.

The small fraction of Na^+ in *tf*-FeZSM-5 was exchanged for NH_4^+, which subsequently was converted in H^+ by calcination in dry air so that the proton form (*H*-FeZSM-5) was obtained. Upon ion exchange and calcination, essentially as the result of changing the charge-compensating cation from Na^+ to NH_4^+ and finally to H^+, the symmetry of iron in the framework further deviates from T_d geometry. While a flow of dried air was used during the calcination, it is not likely that iron is really extracted from the framework. Most probably the elongation of one of the Fe−O bonds in the FeO_4 unit causes the distortion of the pure tetrahedral site. The longer Fe−O bond can be attributed to the formation of a bridging hydroxyl bond, Fe−O(H)−Si, due to the association of a proton to oxygen in the Fe−O−Si bond. This phenomenon was earlier observed by using EXAFS for a high-loaded, framework-substituted FeZSM-5 with an Fe content of 3.98 wt % and almost no Al in it.[33] For that catalyst it was also shown that the normal tetrahedral environment could be restored upon introduction of other monovalent ions such as Na^+ or K^+.[34]

4.3. Steam Treatment. The influence of deliberate disruption of Fe−O−Si bonds by heating in a helium stream containing water vapor (steaming) on the iron coordination was investigated for *H*-FeZSM-5. The method used in the literature[4] is the hard-steaming procedure, with a water partial pressure of 300 mbar in a total flow of 30 mL/min of nitrogen at a high temperature of 600 °C for 5 h. Hard steaming causes considerable extraction of iron out of the framework. Using the above outlined quantification method, based on the integrated pre-edge intensities of the Fe^{III} references, we determined that just 19% of the iron is left in the tetrahedral positions of the framework.

Separately, we performed a mild-steaming procedure with a water partial pressure of 200 mbar in a total flow of 200 mL/min of nitrogen at a high temperature of 550 °C for 4 h. In that case 32% of the iron is present in framework positions, compared to 19% for the hard-steamed sample. So, the decrease of the amount of iron in tetrahedral framework positions is related to the duration and severity of the steaming procedure, where the pre-edge intensity is lower for hard-steamed (*hs*) compared to mild-steamed (*ms*) samples.

It is likely that the effort to extract iron out of the zeolite matrix increases with the decreasing fraction of tetrahedral iron left. Even after a severe steaming treatment a significant fraction of iron stays in the framework (19%). Although the substitution of Si by Fe is rather low (Si/Fe ratio ∼ 360) the presence of extraframework Fe will hinder the extraction of underlying framework iron. Most likely there is a large variety in the extracted iron species based on the nearly symmetric shape of the pre-edge peak. The presence of purely octahedrally coordinated iron species would have given rise to a typical shoulder in the pre-edge feature at higher energy (cf. Fe_2O_3 in Figure 3). Thus, probably the extracted iron did not fully agglomerate into stable iron oxide species with fixed octahedral coordination.

4.4. Stabilization of Extraframework Fe. The role of aluminum in the MFI structure on the extraction of iron by

steaming is not yet clear. Lamberti and co-workers reported for Fe-silicalite the dislodgement of iron out of the zeolite matrix upon a template removal at 500 °C and activation in vacuum at 700 °C. A significant fraction of iron was supposed to be in extraframework positions and could be reduced. Pirutko et al.[35] investigated the activity of iron centers (α-sites) of several steamed MFI catalysts for the benzene to phenol oxidation and found a nonlinear correlation between the total amount of iron and the active part. Catalysts displaying strong Brönsted acidity (containing either Al or Ga) were much more active than others (containing B or Ti). Peréz-Ramírez et al.[36] investigated the evolution of iron species and activity in the direct N_2O decomposition for steam-activated Fe-MFI zeolites. They claimed that the stability of Fe-silicalite is higher than for Fe-AlZSM-5 and Fe-GaZSM-5, due to the destabilizing effect of Ga and Al on Fe−O−Si bonds. Their conclusion is based on the lower temperature of the steaming treatment needed for the optimum activity in the case of the Al- and Ga-containing Fe-MFI.

A major problem, however, is the difficulty in determining the degree of extraction of iron. A lower activity does not necessarily mean a lower extent of extraction but can also point to a higher degree of agglomeration. A statistical analysis of infrared data of NO absorption on Fe-silicalite and FeZSM-5 samples by the group of Lamberti revealed that the presence of framework Al favors the dispersion of extraframework Fe centers.[37,38] In summary, the extraction of Fe from the zeolite framework might be easier in the case of aluminum-containing Fe-MFI samples, but the resistance toward the formation of larger clusters is most likely higher. In this view, it is not surprising that for our framework-substituted FeZSM-5 samples the iron is pulled out of the zeolite lattice to form extraframework iron upon the progressive treatments. On the other hand, we did not see the formation of a dominant amount of Fe_2O_3-like iron species even after performing a steaming treatment.

4.5. Coordination of Water. The presence of Fe^{III} in a distorted octahedral 5-fold coordination by oxygen atoms is observed for binuclear iron clusters in over-exchanged *cvd*-Fe/ZSM-5 in oxygen (50% in helium) at 350 °C.[8] We measured the same sample with Kβ-detected XANES and found also an integrated pre-edge intensity corresponding to an Fe coordination of on average five in 7.7% oxygen in helium. This means that most of the iron is present in binuclear clusters and that the oxygen bridge is predominantly intact, where on each Fe atom a water group is missing. On the subsequent lowering of the temperature from 350 to 25 °C the H_2O is again able to coordinate to the iron, making up the octahedral arrangement. The change from mainly tetrahedrally coordinated iron to octahedral coordination upon cooling to room temperature is even more pronounced for calcined framework-substituted *H*-FeZSM-5. In this case, two water molecules may be bonded to one iron atom that is still in the zeolite framework. Some water is always present in the zeolite channels and cages, and upon lowering the temperature it becomes favorable to bind to the iron species.

4.6. Outlook. Our study of the nature of Fe sites in FeZSM-5 zeolites demonstrates the strengths of selective X-ray absorption techniques such as Kβ-detected XANES. It introduces a new, more accurate technique to quantitatively determine the oxidation state and coordination of transition metal ions in catalysts, even when the loading is below 1 wt %. High-resolution spectra with a small background and a good separation of the pre-edge feature from the main edge make Kβ-detected XANES a valuable tool for chemical research, including biological systems.

5. Conclusions

Kβ-detected XANES has been used to study framework-substituted FeZSM-5 zeolites. For the first time a quantitative analysis of XANES data was presented on an FeZSM-5 catalyst with an Fe loading fairly well below 1 wt %. This achievement is not only a technical breakthrough in X-ray absorption spectroscopy applied to catalysis but it opens new possibilities to study in detail the active site of low-loaded, framework-substituted FeZSM-5 zeolites, which have an Fe content similar to catalysts used for the industrial conversion of benzene to phenol.[1]

The application of this new technique to FeZSM-5 and related iron oxide model compounds revealed that Kβ-detected XANES allows for a quantitative investigation of the oxidation state and local coordination of transition metal ions in catalysis under *in situ* conditions. The main improvement is due to high-resolution spectra with a significantly smaller background contribution to the pre-edge feature.

The removal of the synthesis template from FeZSM-5 zeolites by heating is practically impossible without introducing minor changes in the elemental composition and local geometry of the framework, although the major structure might not be affected.

The (deliberate) presence of water during heat treatments of framework-substituted FeZSM-5 causes the breaking of Fe−O−Si bonds and results in the formation of extraframework Fe species. The degree of iron extraction is dependent on the duration and severity of the steam treatment. No evidence is found for the predominant presence of ordered iron oxide phases.

Acknowledgment. The authors thank the BioCAT and Advanced Photon Source staff for their support during the measurements at Argonne National Laboratories. Use of the APS was supported by the U.S. Department of Energy, Basic Energy Sciences, Office of Science, under Contract No. W-31-109-ENG-38. BioCAT is a National Institutes of Health-supported Research Center RR-08630. We thank C. P. Baldé (Utrecht University) for assisting with the sample treatments of the framework-substituted FeZSM-5 zeolites and Dr. A. A. Battiston (Utrecht University) for the preparation of the over-exchanged *cvd*-Fe/ZSM-5 samples. Dr. P. A. van Aken (Technical University Darmstadt) is gratefully acknowledged for kindly providing the Fayalite sample. The research of W.M.H. and P.G. is supported by Grants (respectively 700.98.036 and 016.022.002) from the Netherlands Scientific Organization-Chemical-Sciences (NWO-CW). The research of F.M.F.dG. is supported by the Netherlands Research School Combination on Catalysis (NRSCC) and by a Science-Renewal Fund 016.022.002 of NWO-CW. U.B. was supported by the Stanford Synchrotron Radiation Laboratory, Department of Energy, Office of Basic Energy Sciences Contract DE-AC03-765F00575.

References and Notes

(1) Panov, G. I. *CATTECH* **2000**, *4*, 18−32.

(2) Panov, G. I.; Uriarte, A. K.; Rodkin, M. A.; Sobolev, V. I. *Catal. Today* **1998**, *41*, 365−385.

(3) Pérez-Ramírez, J.; Mul, G.; Kapteijn, F.; Moulijn, J. A.; Overweg, A. R.; Doménech, A.; Ribera, A.; Arends, I. W. C. E. *J. Catal.* **2002**, 113−126.

(4) Ribera, A.; Arends, I.; De Vries, S.; Perez-Ramirez, J.; Sheldon, R. A. *J. Catal.* **2000**, *195*, 287−297.

(5) Chen, H. Y.; Sachtler, W. M. H. *Catal. Today* **1998**, *42*, 73−83.

(6) Zhu, Q.; Mojet, B. L.; Janssen, R. A. J.; Hensen, E. J. M.; Van Grondelle, J.; Magusin, P.; Van Santen, R. A. *Catal. Lett.* **2002**, *81*, 205−212.

(7) Sun, Q.; Gao, Z. X.; Chen, H. Y.; Sachtler, W. M. H. *J. Catal.* **2001**, *201*, 89−99.

(8) Battiston, A. A.; Bitter, J. H.; De Groot, F. M. F.; Overweg, A. R.; Stephan, O.; Van Bokhoven, J. A.; Kooyman, P. J.; Van Der Spek, C.; Vanko, G.; Koningsberger, D. C. *J. Catal.* **2003**, *213*, 251−271.

(9) Marturano, P.; Drozdova, L.; Pirngruber, G. D.; Kogelbauer, A.; Prins, R. *Phys. Chem. Chem. Phys.* **2001**, *3*, 5585−5595.

(10) Groothaert, M. H.; van Bokhoven, J. A.; Battiston, A. A.; Weckhuysen, B. M.; Schoonheydt, R. A. *J. Am. Chem. Soc.* **2003**, *125*, 7629−7640.

(11) Prestipino, C.; Bordiga, S.; Lamberti, C.; Vidotto, S.; Garilli, M.; Cremaschi, B.; Marsella, A.; Leofanti, G.; Fisicaro, P.; Spoto, G.; Zecchina, A. *J. Phys. Chem. B* **2003**, *107*, 5022−5030.

(12) Westre, T. E.; Kennepohl, P.; Dewitt, J. G.; Hedman, B.; Hodgson, K. O.; Solomon, E. I. *J. Am. Chem. Soc.* **1997**, *119*, 6297−6314.

(13) Joyner, R.; Stockenhuber, M. *J. Phys. Chem. B* **1999**, *103*, 5963−5976.

(14) Heinrich, F.; Schmidt, C.; Loffler, E.; Menzel, M.; Grunert, W. *J. Catal.* **2002**, *212*, 157−172.

(15) Jia, J. F.; Sun, Q.; Wen, B.; Chen, L. X.; Sachtler, W. M. H. *Catal. Lett.* **2002**, *82*, 7−11.

(16) Chen, H. Y.; El-Malki, E. M.; Wang, X.; Van Santen, R. A.; Sachtler, W. M. H. *J. Mol. Catal. A* **2000**, *162*, 159−174.

(17) Bordiga, S.; Buzzoni, R.; Geobaldo, F.; Lamberti, C.; Giamello, E.; Zecchina, A.; Leofanti, G.; Petrini, G.; Tozzola, G.; Vlaic, G. *J. Catal.* **1996**, *158*, 486-501.

(18) Berlier, G.; Spoto, G.; Bordiga, S.; Ricchiardi, G.; Fisicaro, P.; Zecchina, A.; Rossetti, I.; Selli, E.; Forni, L.; Giamello, E.; Lamberti, C. *J. Catal.* **2002**, *208*, 64−82.

(19) Ferretti, A. M.; Oliva, C.; Forni, L.; Berlier, G.; Zecchina, A.; Lamberti, C. *J. Catal.* **2002**, *208*, 83−88.

(20) Berlier, G.; Spoto, G.; Fisicaro, P.; Bordiga, S.; Zecchina, A.; Giamello, E.; Lamberti, C. *Microchem. J.* **2002**, *71*, 101−116.

(21) Zecchina, A.; Bordiga, S.; Spoto, G.; Damin, A.; Berlier, G.; Bonino, F.; Prestipino, C.; Lamberti, C. *Top. Catal.* **2002**, *21*, 67−78.

(22) Wilke, M.; Farges, F.; Petit, P. E.; Brown, G. E.; Martin, F. *Am. Mineral.* **2001**, *86*, 714−730.

(23) Battiston, A. A.; Bitter, J. H.; Heijboer, W. M.; De Groot, F. M. F.; Koningsberger, D. C. *J. Catal.* **2003**, *215*, 279−293.

(24) Battiston, A. A.; Bitter, J. H.; Koningsberger, D. C. *J. Catal.* **2003**, *218*, 163−177.

(25) Hamalainen, K.; Siddons, D. P.; Hastings, J. B.; Berman, L. E. *Phys. Rev. Lett.* **1991**, *67*, 2850−2853.

(26) Caliebe, W. A.; Kao, C. C.; Hastings, J. B.; Taguchi, M.; Uozumi, T.; de Groot, F. M. F. *Phys. Rev. B* **1998**, *58*, 13452−13458.

(27) de Groot, F. M. F. *Chem. Rev.* **2001**, *101*, 1779−1808.

(28) Bergmann, U.; Cramer, S. P. *Proc. SPIE* **1998**, *3448*, 198−209.

(29) Vaarkamp, M.; Mojet, B. L.; Kappers, M. J.; Miller, J. T.; Koningsberger, D. C. *J. Phys. Chem.* **1995**, *99*, 16067−16075.

(30) Wong, J.; Lytle, F. W.; Messmer, R. P.; Maylotte, D. H. *Phys. Rev. B* **1984**, *30*, 5596.

(31) Verberckmoes, A. A.; Weckhuysen, B. M.; Schoonheydt, R. A. *Microporous Mesoporous Mater.* **1998**, *22*, 165−178.

(32) Milanesio, M.; Artioli, G.; Gualtieri, A. F.; Palin, L.; Lamberti, C. *J. Am. Chem. Soc.* **2003**, *125*, 14549−14558.

(33) Axon, S. A.; Fox, K. K.; Carr, S. W.; Klinowski, J. *Chem. Phys. Lett.* **1992**, *189*, 1−6.

(34) Sankar, G.; Thomas, J. M.; Catlow, C. R. A. *Top. Catal.* **2000**, *10*, 255−264.

(35) Pirutko, L. V.; Chernyavsky, V. S.; Uriarte, A. K.; Panov, G. I. *Appl. Catal. A* **2002**, *227*, 143−157.

(36) Perez-Ramirez, J.; Kapteijn, F.; Groen, J. C.; Domenech, A.; Mul, G.; Moulijn, J. A. *J. Catal.* **2003**, *214*, 33−45.

(37) Berlier, G.; Zecchina, A.; Spoto, G.; Ricchiardi, G.; Bordiga, S.; Lamberti, C. *J. Catal.* **2003**, *215*, 264−270.

(38) Berlier, G.; Bonino, F.; Zecchina, A.; Bordiga, S.; Lamberti, C. *ChemPhysChem.* **2003**, *4*, 1073−1078.